Species mobility induces synchronization in chaotic population dynamics

N. Kouvaris,[1,2,*] D. Kugiumtzis,[2] and A. Provata[1]

[1]*Institute of Physical Chemistry, National Center for Scientific Research "Demokritos," G-15310 Athens, Greece*

[2]*Department of Mathematical, Physical and Computational Sciences, Faculty of Engineering, Aristotle University of Thessaloniki, G-54124 Thessaloniki, Greece*

(Received 28 March 2011; published 22 September 2011)

A prototype population dynamics model with cyclic domination of four species and empty sites is proposed for studying transition to synchronization. At the mean-field level the dynamics shows quasiperiodicity and chaos depending on the parameter values. The realization of the model on a square lattice shows that spatial restrictions and intrinsic stochasticity change the whole picture. The mean-field dynamics qualitatively remains only under global reactions, while local reactions drive the lattice to poisoning, where only some of the species survive. Nontrivial oscillatory steady states are developed if long-distance exchange is introduced due to gradual mixing with a certain probability. The mixing probability is shown to control the transition to synchronization which emerges abruptly following a phase slip scenario. Near the transition a typical intermittency crisis takes place, with phase slips becoming more infrequent as the transition is approached.

DOI: 10.1103/PhysRevE.84.036211 PACS number(s): 05.45.Xt, 02.50.Ey, 05.10.Ln, 87.23.Cc

I. INTRODUCTION

Synchronization of locally reacting elements, in the onset of rhythmic behavior of individuals and bulk oscillations, constitutes one of the most interesting and widespread phenomena in complex systems [1,2]. In biological and ecological systems, synchronization is also a frequent feature. Oscillations in prey-predator systems [3] or in populations of coupled stochastic discrete-state units [4,5], rhythmic disease spreading in epidemiological models [6,7], the appearance of limit cycles [8], and domain synchronization [9] in a cyclic Lotka Volterra model are only some examples of the diverse disciplines where the signature of synchronization is intense. Successful models like Kuramoto phase oscillators [10] and Vicsek self-propelled particles [11] have also been introduced in studies of collective motion inducing synchronization in large sets of biological populations.

A common principle of such systems is the spatial distribution of a finite number of individuals which interact locally within their neighborhood. The local interactions induce spatial correlations and designate the failure of mean-field (MF) models, which, however, can describe the macroscopic behavior. An additional considerable feature in reactive dynamics is the mobility of species, which mixes spatially separated groups [12]. For real ecosystems it is known that mobility is an inclusive attribute that is common from bacteria swarming [13] to the collective motion of birds [14] and animal migration [3]. In recent studies [8,15–17] this mobility has been considered a diffusive mixing mechanism which compensates for the locality of spatial interactions. In other words, long-distance exchange plays the role of a coupling mechanism between distant neighborhoods of the system. The evolution of the system depends strongly on the combination of reaction and long-distance exchange processes.

In previous works the authors have studied an interacting population model with cyclic domination of two species (predator and prey) and empty sites which is governed by conservative, center-type dynamics in the MF description [16,17]. In [16] and [17], the system shows periodic oscillations around an elliptic equilibrium point (center) in the MF approach. Stochastic simulations showed that the cooperation between the local dynamics and the long-distance coupling mechanism causes a transition to synchronization of populations between different neighborhoods of the reaction network. The role of species mobility (migration over long distances) in the two-species model has been analyzed in [16]. In the current study we extend the above concepts to a multispecies model with more complex or even chaotic dynamics. Mobility-mixing processes are also investigated in such ecosystems.

In recent experiments [18], evidence of deterministic chaos has been observed in real trophic webs. Furthermore, deterministic chaos at the MF level has been theoretically investigated for multispecies food chain models [19], considering that two predators consume the same prey or other types of species interactions. Nevertheless, to understand the interplay of global versus local environmental factors and the influence of species mobility, further theoretical studies are needed in these directions, as well as studies of synchronization. Toward this purpose, we introduce a multispecies ecosystem which exhibits deterministic chaos at the MF level. The analytical MF approach assuming an infinite number of homogeneously mixed populations is presented in order to give a macroscopic picture of the system. Nevertheless, the main purpose of this work is the study of synchronization when the system is realized on a square lattice with kinetic Monte Carlo (KMC) simulations. Particularly, synchronization is studied in two situations. In the first case all species can react with all other species independently of the distance between them. The dynamics here is qualitatively well described by the MF theory. In the second case the species react only locally and they can exchange their position with a certain probability p_{ex}. The latter process stands for a gradually mixing mechanism. Synchronization here arises as a function of this exchange probability p_{ex} or as a function of the mixing distance r_{ex}.

As shown in the sequel, local KMC simulations of the current multispecies model always lead to poisoning states, i.e., to

*nkoub@chem.demokritos.gr

states where only some of the species survive. This is different from the two-species model [16], where nonpoisoning states are a common feature, even in the absence of global coupling. It is shown in the next sections that for multispecies models the role of long-distance (and global) reaction or diffusion processes is crucial because they drive the system away from poisoning states. In this case a species equilibrium is achieved with the presence of all interacting species.

The current work is organized as follows. In Sec. II the reactive model is briefly presented, while its MF deterministic dynamics is worked out in detail in Sec. III. Power spectra and Lyapunov exponents are used to characterize the quasiperiodic and chaotic dynamics. In Sec. IV the stochastic dynamics of the model is studied. Local reactions and fluctuations are taken into account in a Master equation approach which is solved with KMC simulations. Finally, a gradually mixing step is added to the reactive scheme and allows for long-distance species mobility. The degree of mobility is determined by the exchange probability $p_{\rm ex}$ and the maximum exchange distance $r_{\rm ex}$. The interplay of mobility with local dynamics can drive the system to synchronization, which is studied both qualitatively and quantitatively. In Sec. V a short discussion briefly recapitulates the main aspects of this system.

II. THE MODEL

From the previous discussion it becomes evident that the proposed kinetic scheme needs to fulfill the following two criteria: (a) it must exhibit chaotic dynamics at the MF level, and (b) it must be lattice compatible due to its implementation on a lattice by stochastic KMC simulations [16]. Although it is easy to find kinetic schemes that meet each one of the two criteria separately, very few schemes satisfy both of them at the same time. The proposed scheme was chosen as a representative, simple example in the class of schemes that fulfill both requirements.

The kinetic model contains four interacting species, X, Y, Z, and U taking part in a series of trimolecular and bimolecular reactions on an underlying lattice network. The network is represented by a regular square lattice containing a constant number of sites. Each site can be occupied by only one species or can be empty (denoted S). Thus empty sites S are considered virtual species, allowing for a lattice implementation of the model. Within this picture, every lattice site can be found in any of the five possible states $\{X,Y,Z,U,S\}$. The interactive scheme is given by

$$X + 2Y \xrightarrow{k_1} 3Y, \tag{1a}$$

$$2Y + Z \xrightarrow{k_2} 3Z, \tag{1b}$$

$$Z + U \xrightarrow{k_3} 2U, \tag{1c}$$

$$U + S \xrightarrow{k_4} 2S, \tag{1d}$$

$$S + X \xrightarrow{k_5} 2X, \tag{1e}$$

where the parameters k_i, $i = 1 \ldots 5$, are the transition probabilities of the corresponding reaction processes. All five reactions have self-feedback and the whole process represents a chain of prey-predator interactions. In process (1a) two predators Y give birth to a third one by consuming a prey X. In process (1b) two species Y become prey and are consumed by the new predator Z. In the bimolecular process (1c) a species Z becomes prey and is consumed by the new predator U. This new predator dies in the absence of prey, as defined in process (1d). The chain is completed with the birth of a new species X in an empty site, given in process (1e).

III. MEAN-FIELD DETERMINISTIC APPROACH

In the following the MF theory of system (1) is presented with some analytical results and numerical arguments. In this approach each individual element interacts with the MF of all the others and the interaction does not depend on the distance between them. The MF approach focuses on the macroscopic features of the system, which may be used for comparison with the KMC simulations. Fluctuations are neglected in this description, which characterizes the macroscopic deterministic dynamics of the system (1). The time evolution of the concentrations x,y,z,u,s of the species X,Y,Z,U and empty sites S, respectively, can be described by the rate equations

$$\dot{x} = k_5 xs - k_1 xy^2, \tag{2a}$$

$$\dot{y} = k_1 xy^2 - 2k_2 y^2 z, \tag{2b}$$

$$\dot{z} = 2k_2 y^2 z - k_3 uz, \tag{2c}$$

$$\dot{u} = k_3 uz - k_4 us, \tag{2d}$$

$$\dot{s} = k_4 us - k_5 sx, \tag{2e}$$

which contain all the dynamical features of the system. These equations describe a homogeneous and isotropic system, without spatial correlations [20]. It is obvious already, from the initial scheme, (1), that the total number of individual species and empty sites is conserved, which is a property correctly reproduced by the rate equations, (2). The corresponding constant of motion reads

$$C_1 = x + y + z + u + s. \tag{3}$$

By setting the constant $C_1 = 1$ the dynamical variables x,y,z,u,s represent the partial concentrations of the corresponding species. Using Eq. (3), the dimensionality can be reduced and the system dynamics can be displayed in a four-dimensional phase space written in terms of x,y,z,u (if $s = 1 - x - y - z - u$). The reduced system is given by the equations

$$\dot{x} = -k_1 xy^2 + k_5 x(1 - x - y - u - z), \tag{4a}$$

$$\dot{y} = k_1 xy^2 - 2k_2 y^2 z, \tag{4b}$$

$$\dot{z} = 2k_2 y^2 z - k_3 uz, \tag{4c}$$

$$\dot{u} = k_3 uz - k_4 u(1 - x - y - u - z). \tag{4d}$$

The reduced system, (4), has one more constant of motion:

$$C_2 = \ln[x^{2k_2k_4} z^{k_1k_4} u^{2k_2k_5} (1 - x - y - z - u)^{k_1k_3}] - k_3k_5/y. \tag{5}$$

Expressions (3) and (5) are invariant with respect to time. Equation (3) reflects the lattice restriction, which dictates that the number of lattice sites, empty or occupied, is conserved. Equation (5) shows the conservation of the expression C_2, but it does not have a direct energy-like physical analog.

In the following the parameters $k_i, i = 1 \ldots 5$, are restricted to positive values, since they represent transition probabilities. The dynamical variables x, y, z, u, s are positive and less than unity, as they represent the relative concentrations of species:

$$0 \leqslant x; \quad 0 \leqslant y; \quad 0 \leqslant z; \quad 0 \leqslant u; \quad x + y + z + u \leqslant 1. \tag{6}$$

The closed contour bounding region, (6), determines the invariant manifolds of the reduced system

$$x = 0; \quad y = 0; \quad z = 0; \quad u = 0; \quad x + y + z + u = 1. \tag{7}$$

Hence, choosing the initial values inside the bounded region, (6), the trajectories will always be bounded. The reduced system, (4), has five equilibrium subsets of the manifolds, (7), and two equilibrium points in the interior of these sets.

One trivial equilibrium point is

$P_1 = (0; 0; 0; 0)$ with eigenvalues $[0; 0; -k_4; k_5]$. This point is located on the intersection of the four invariant manifolds and represents the annihilation of the four species.

One nontrivial equilibrium point is

$P_2 = (\frac{K_1 - \sqrt{K_2}}{K_3}; \frac{2K_4}{K_4 + \sqrt{K_2}}; \frac{k_1(K_1 - \sqrt{K_2})}{2k_2K_3}; \frac{k_5(K_1 - \sqrt{K_2})}{k_4K_3})$, where $K_1 = k_2k_4(2k_1(k_3 + k_4) + k_3k_5 + 4k_2(k_4 + k_5))$, $K_2 = k_2^2k_3k_4^2k_5(4k_1(k_3 + k_4) + k_3k_5 + 8k_2(k_4 + k_5))$, $K_3 = (k_1(k_3 + k_4) + 2k_2(k_4 + k_5))^2$, and $K_4 = k_2k_3k_4k_5$. This point is located inside the bounded region and has purely imaginary, per two conjugate eigenvalues. Its coordinates determine the average concentrations of species within the phase space. The five equilibria sets are

(i) $P_3 = (x; 0; 1 - x; 0)$, with eigenvalues $[0; 0; k_3(1 - x); -k_5x]$.

(ii) $P_4 = (x; 0; 0; 1 - x)$, with eigenvalues $[0; 0; -k_3(1 - x); k_4 - (k_4 + k_5)x]$. This point changes its stability on $x^{\mathrm{cr}} = k_4/(k_4 + k_5)$.

(iii) $P_5 = (0; y; 0; 1 - y)$, with eigenvalues $[0; k_4(1 - y); -k_1y^2; -k_3(1 - y) + 2k_2y^2]$. This point changes its stability on $y^{\mathrm{cr}} = (-k_3 \pm \sqrt{k_3(8k_2 + k_3)}/(4k_2)$.

(iv) $P_6 = (1 - z; 0; z; 0)$, with eigenvalues $[0; 0; -k_5(1 - z); k_3z]$.

(v) $P_7 = (1 - u; 0; 0; u)$, with eigenvalues $[0; 0; -k_3u; -k_5 + (k_4 + k_5)u]$. This point changes its stability on $u^{\mathrm{cr}} = k_5/(k_4 + k_5)$.

Each of these five lines represents the survival of only two among four species, while the other two die out. The competition between these two surviving species, if it is allowed by the initial scheme, may finally cause the domination of only one and the annihilation of the other.

Besides the above equilibrium points and their linear stability it is important to study the whole phase space of the system. The phase space study, the Poincaré sections, and the Lyapunov exponent analysis are helpful in the comparison with KMC simulations presented in the next section.

The phase trajectories are wrapped around the nontrivial equilibrium point P_2 and they evolve inside the absorbing boundary (6). This means that the dynamical variables x, y, z, u revolve around P_2, thus the species population follows a corresponding cyclic behavior.

As shown in Fig. 1 the system demonstrates both ordered and chaotic trajectories. This is depicted in the Poincaré sections. For low values of k_4 the Poincaré sections point to a regime where the flow trajectories lie on a toroidal surface embedded in the four-dimensional phase space. For larger values of k_4 it reaches a chaotic regime. It is clearly shown that by increasing the parameter k_4 the trajectories become more dense in phase space. The parameter value $k_4 = 0.2$ produces an ordered trajectory with a very thin trace on the Poincaré section. For $k_4 = 0.3$ the trajectory is weakly chaotic and its trace on the surface of Poincaré section is wider. For $k_4 = 0.31$ the chaotic behavior is more pronounced, however, stability islands are still shown on the section. Finally, for $k_4 = 0.7$ the trajectory is fully chaotic and all the stability islands have been destroyed.

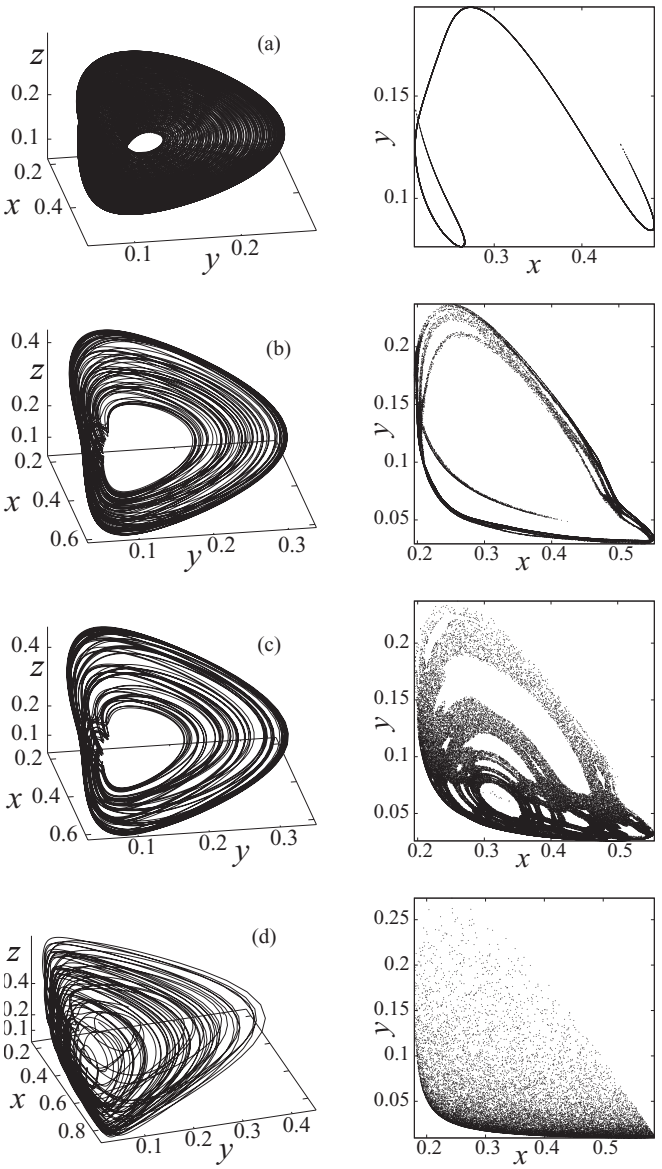

FIG. 1. Transition from quasiperiodic to chaotic oscillations. Left: Projections of trajectories of the reduced system, (4), on the x-y-z phase space. Right: Projections of the corresponding Poincaré sections on the x-y plane. From top to bottom the parameter k_4 takes the values (a) 0.2, (b) 0.3, (c) 0.31, and (d) 0.7. The other parameters are $k_1 = k_2 = 0.7$ and $k_3 = k_5 = 0.1$. Initial conditions are $x_0 = y_0 = z_0 = u_0 = 0.2$.

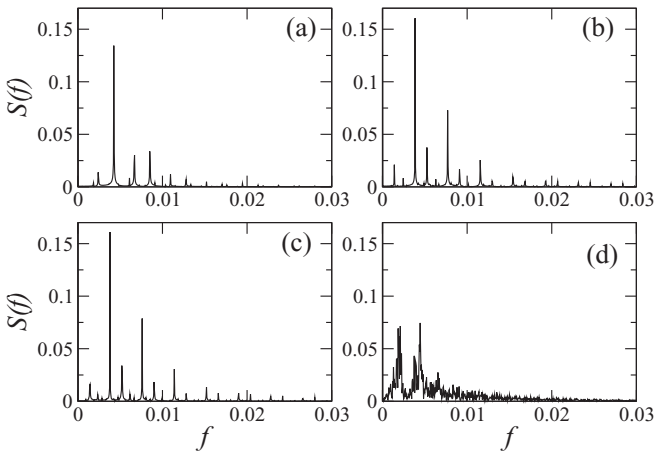

FIG. 2. Power spectral density of trajectories presented in Fig. 1. The parameter k_4 takes the values (a) 0.2, (b) 0.3, (c) 0.31, and (d) 0.7. The remaining parameters are the same as in Fig. 1.

A detailed view of the power spectral density $S(f)$ of these trajectories (as projected on the axis of the variable x) indicates that the system follows a quasiperiodic route to chaos. In Fig. 2(a), for the parameter value $k_4 = 0.2$, in addition to the main frequency and its harmonics, a series of other frequencies and their sums is observed. This indicates that the corresponding toroidal in Fig. 1(a) represents a quasiperiodic trajectory. For a larger value of parameter $k_4 = 0.3$ [Fig. 2(b)], the spectrum acquires more power at higher frequencies. Increasing the parameter further, to the value $k_4 = 0.31$, these secondary frequencies become more pronounced and even more new frequencies emerge. Finally, for $k_4 = 0.7$, $S(f)$ becomes continuous [Fig. 2(d)], indicating a chaotic trajectory.

The dynamical stability of the trajectories presented in Fig. 1 can be quantitatively identified by calculating the maximum Lyapunov exponent λ_1, which gives the rate of exponential divergence from perturbed initial conditions. The calculated λ_1 of the corresponding trajectories is presented on a logarithmic scale in Fig. 3 . It has already been mentioned that the parameter $k_4 = 0.2$ points to a quasiperiodic trajectory. This is confirmed by λ_1, which tends to 0 as time goes to

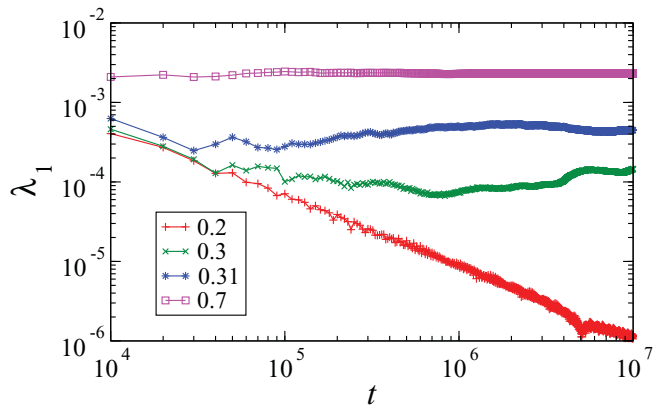

FIG. 3. (Color online) Maximum Lyapunov exponent of the trajectories presented in Fig. 1. The corresponding parameter k_4 is shown in the legend. The remaining parameters are the same as in Fig. 1.

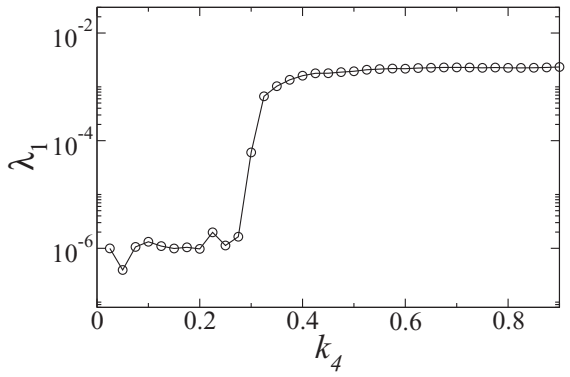

FIG. 4. Maximum Lyapunov exponent as a function of parameter k_4, calculated for $t = 10^7$ time steps. The remaining parameters are the same as in Fig. 1.

infinity. The other values of k_4 in Fig. 3 correspond to weak or full chaos and thus λ_1 tends to positive values. Larger positive values indicate further developed chaos within the time interval of the numerical calculations (10^7 time steps). However, there is a plateau where λ_1 takes values of the same order of magnitude. This plateau is reached after a transition from zero values [$O(10^{-6})$] of λ_1, as shown in Fig. 4 .

The above MF description of system (1) shows that the multispecies prey-predator system demonstrates quasiperiodic and chaotic behavior as a function of the control parameter k_4. Qualitatively similar behavior is also observed for the other parameters k_i. In the next section we investigate the deviation in the behavior of this system from the MF when spatial restrictions of the reaction rules and fluctuations are taken into account.

IV. KINETIC MONTE CARLO SIMULATIONS

At the microscopic level, the probability $P_{\boldsymbol{\eta}}$ of finding the system in a configuration $\boldsymbol{\eta}$ is determined by the Master equation,

$$\frac{d}{dt}P_{\boldsymbol{\eta}} = \sum_{\boldsymbol{\eta}'}(W_{\boldsymbol{\eta}'\to\boldsymbol{\eta}}P_{\boldsymbol{\eta}'} - W_{\boldsymbol{\eta}\to\boldsymbol{\eta}'}P_{\boldsymbol{\eta}}). \tag{8}$$

In Eq. (8) $\boldsymbol{\eta},\boldsymbol{\eta}'$ are two different lattice configurations, $W_{\boldsymbol{\eta}'\to\boldsymbol{\eta}}$ and $W_{\boldsymbol{\eta}\to\boldsymbol{\eta}'}$ are the rates of transition $\boldsymbol{\eta}' \to \boldsymbol{\eta}$ and $\boldsymbol{\eta} \to \boldsymbol{\eta}'$, respectively, and the sum is over all possible configurations. Each configuration is given by a vector

$$\boldsymbol{\eta} = H_{1,1}, H_{1,2} \ldots H_{1,L}; \ldots H_{i,j} \ldots H_{i,L}; \ldots H_{i+1,j} \ldots; \times \ldots H_{L,L}, \tag{9}$$

where the element $H_{i,j}$, with $\{i,j\} = 1 \ldots L$, stands for the state of lattice site (i,j). The lattice has linear size L and the variable $H_{i,j}$ can take values from the set of states $\{X,Y,Z,U,S\}$. The description of this problem needs a complicated nonlinear Master equation, which makes its solution a hard task or even impossible. Thus KMC simulations are employed on a square $L \times L$ lattice, where the local environment can be exactly specified and stochastic local reactions can be directly simulated from the initial scheme. KMC is a way to solve the Master equation and consists of the following steps for the cyclic sequence of species

obeying (1):

(1) A lattice site (i,j) is randomly chosen.

(2) If site (i,j) contains a species X or a species Y, then two additional nearest-neighbor sites are randomly selected.

- (a) If the original site (i,j) contains a species X and both the neighbors contain species Y, step (1a) takes place. Namely, site (i,j) changes its state from X to Y with transition probability k_1.
- (b) If the original site (i,j) contains a species Y and one of the neighbors contains a species Y while the other contains a species Z, then both sites containing Y species change their state from Y to Z with probability k_2 [step (1b)].

(3) If site (i,j) contains a species Z or U or is empty, then one neighbor site is also selected.

- (a) If site (i,j) contains a species Z and the selected neighbor site contains a species U, then the site (i,j) changes its state from Z to U with probability k_3 [step (1c)].
- (b) If the original site (i,j) contains a species U and the selected neighbor site is empty, then the desorption (1d) takes place with probability k_4.
- (c) If the original site (i,j) is empty and the selected neighbor site contains a species X, then a second X can adsorb on the selected empty site with probability k_5 via the adsorption step (1e).

The algorithm above describes the local reactions occurring in one elementary time step (ETS). In our simulations one Monte Carlo step (MCS) equals $L \times L$ ETSs. Thus in each MCS, L^2 elementary reactions attempts take place.

Extensive simulations have shown that when only local reactions occur, all possible initial configurations end up as either frozen steady states, which contain a constant number of species and whose contiguity does not allow for further reactions, or poisoning states, where only one species remains. Obviously, the system behaves very differently from the MF because of the local restriction of reactions and the intrinsic randomness of the KMC method. Nevertheless, both approaches show similar behavior when global instead of local reactions take place. Namely, rather than restricting reactions to occur only between neighboring sites, the range of reactivity is expanded to allow species to interact globally with all other species within the whole lattice. The simulation algorithm remains the same, but instead of selecting only nearest-neighboring sites, the "potential neighbors" are equiprobably chosen throughout the whole lattice. This procedure, also referred to as "rewiring" [21–23], constructs an evolving random network which, in qualitative agreement with the MF, can exhibit chaotic dynamics, as shown in Fig. 5. In both figures the power spectral density shows two main frequencies and a continuous background. Of course this agreement is not quantitative, as the time scale is different, and there are fluctuations in the KMC that do not occur in the MF. Quasiperiodic oscillations are also observed in the KMC for different sets of parameters k_i (not presented here). In conclusion, this "all-to-all" reaction mechanism induces phase synchronization and the same chaotic oscillations observed in the whole lattice as well as in small sublattice regions.

We consider an intermediate situation where the species can react locally with a certain probability, and with the complementary probability they choose one or more distant species to react with. This "rewiring" process results in an evolving structure of the lattice substrate. Recent studies [17,22] have shown that this "partial rewiring" constructs a regular "small world" network and, for increasing probability of rewiring, synchronization takes place. Nevertheless, reacting species remain immobile, although they can react even with distant regions. In the following a different mechanism is introduced, which leads to the species mobility and can cause synchronization phenomena.

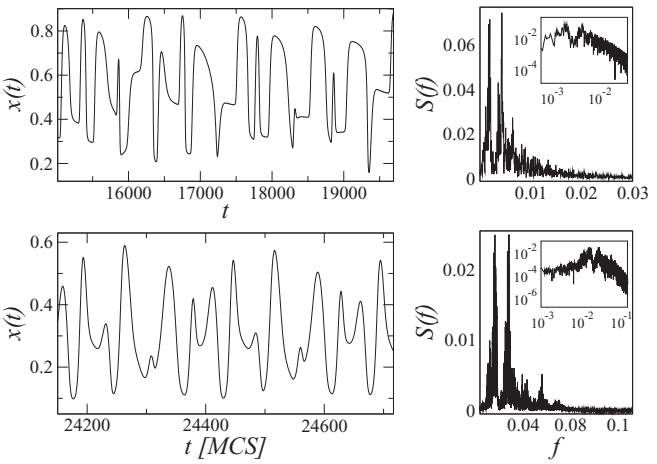

FIG. 5. (Left) The time series of concentration $x(t)$ and (right) the corresponding $S(f)$ on a linear and (inset) logarithmic scale in a chaotic regime calculated from Eqs. (4) (top) and with KMC simulations (bottom). Initial conditions are the same as in Fig. 1 and the parameters are $k_1 = k_2 = k_4 = 0.7$ and $k_3 = k_5 = 0.1$.

As an alternative to all-to-all reactions a different gradually mixing mechanism can counterbalance the effects of purely local reactions. Returning to the initial algorithm, an additional iterative step follows step 1 and reads

(i) A second lattice site (i',j') is randomly selected within a region of maximum exchange radius r_{ex} from the original site (i,j). Then

- (a) with a certain probability p_{ex}, sites (i,j) and (i',j') can instantly exchange their states or
- (b) with the complementary probability $1 - p_{ex}$, steps 2 and 3 of the algorithm (for local reactions) take place.

This process is termed "long-distance exchange" because it refers to exchange between all species. In the case where we only have exchange of species $\{X,Y,Z,U\}$ with empty sites $\{S\}$, this corresponds to "long-distance diffusion" [16,17,27]. Apart from the long-distance exchange, species have the possibility to react locally with the complementary probability. Hence the probability p_{ex}, which is independent of the two site positions, defines the number of exchange attempts over the total number of all attempts. The interplay of this mobility with local reactions induces a threshold in p_{ex} and r_{ex} beyond which species in different areas of lattice are synchronized and bulk oscillations emerge, which coincide in phase and amplitude in different areas. This scenario is illustrated in Fig. 6, where the time evolution of the concentration S species on a slice of the lattice is presented with the corresponding $x(t)$ time series. In these space-time plots, each time a lattice site is empty, a

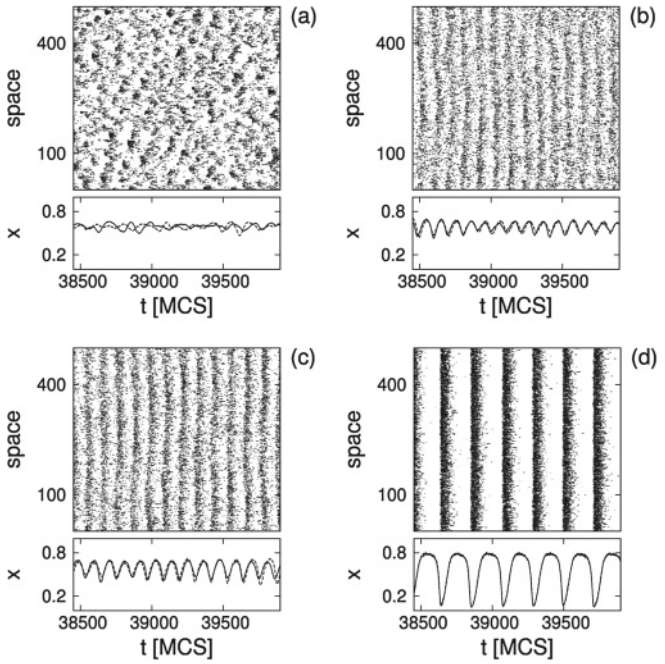

FIG. 6. Transition to synchronization depicted in the evolution of a slice of the lattice. At the top of each panel the space-time plots of the slice are shown, where a black dot is plotted each time a lattice site is empty. The corresponding x concentrations of two distant areas are shown at the bottom of each panel. The long-distance exchange radius is $r_{ex} = 200$ sites and its probability p_{ex} is (a) 0.0003, (b) 0.0012, (c) 0.0014, and (d) 0.01. The initial configuration and remaining parameters are the same as in Fig. 5.

black dot is plotted (only empty sites are plotted for better illustration). Starting from $p_{ex} = 0.0003$ [Fig. 6(a)] the lattice sites change states randomly. Thus each subarea of the lattice exhibits small fluctuations of the species abundance and no bulk oscillations arise. Increasing p_{ex} to larger values the sites start to be empty or occupied in a more coherent way, forming stripe patterns in the space-time plots as shown in Figs. 6(b) and 6(c).

The synchronization is not complete and thus space-time patterns look noisy. Finally, beyond $p_{ex} \approx 0.0025$, distant areas of the lattice are completely synchronized as shown in Fig. 6(d), which induce better coherence between them and thus higher oscillation amplitudes.

The degree of coherence can be characterized using the synchronization index (SI) [1]. Following the analytic signal approach for concentration $x(t)$, measured in regions of 64 lattice sites, the instantaneous phase $\phi(t)$ and the amplitude $Q(t)$ of the measured concentration within a region can be uniquely defined by the analytic signal

$$\zeta(t) = x(t) + i\tilde{x}(t) = Q(t)e^{i\phi(t)}, \tag{10}$$

where the imaginary part $\tilde{x}(t)$ is the Hilbert transform of $x(t)$. Assuming two arbitrary chosen distant regions A and B, each consisting of 64 lattice sites, the phase difference between them is defined as, $\Delta\phi = \phi_A(t) - \phi_B(t)$. Therefrom the SI can be estimated, given by

$$\gamma^2 = \langle\cos(\Delta\phi)\rangle^2 + \langle\sin(\Delta\phi)\rangle^2, \tag{11}$$

which relates in Gaussian approximation to the variance of $\Delta\phi$ distribution. When phases are narrowly distributed around a constant value, the SI goes to unity; otherwise, for broadly distributed phases it goes to 0.

Synchronization can also be confirmed by the mutual information (MI) [24–26]. In recent studies, MI is used as the rate with which information is being exchanged between two oscillation modes or elements in active networks. In those networks the MI and synchronization level increase simultaneously. The maximum of MI is achieved for complete synchronization [27–30].

MI exchange between region A and region B is defined as

$$I(A,B) = \sum_{mn} p_{AB}(m,n) \log \frac{p_{AB}(m,n)}{p_A(m)p_B(n)}, \tag{12}$$

where $p_A(m)$ and $p_B(n)$ are the marginal probability distributions, for appropriate binning of the measured concentration $x(t)$ in regions A and B, respectively, at fixed time intervals (KMC steps). Namely, $p_A(m)$ estimates the frequency of finding an $x(t)$ measurement within region A in bin m, while $p_B(n)$ estimates the frequency of finding an $x(t)$ measurement within region B in bin n. $p_{AB}(m,n)$ is the corresponding joint probability distribution.

In general, MI can be defined as a function of the lag τ, assuming the variables $x_A(t)$ and $x_B(t-\tau)$, i.e., $I(\tau) = I(A_t, B_{t-\tau})$. The estimation of the degree of independence between the subsystems by $I(A_t, B_{t-\tau})$ depends on the choice of τ. In order to suppress this effect the cumulative MI (CMI) is defined by averaging over a range of lags up to a maximum lag τ_{max} [31]:

$$\langle I(A_t, B_{t-\tau})\rangle_\tau = \frac{1}{\tau_{max}+1} \sum_{\tau=0}^{\tau_{max}} I(A_t, B_{t-\tau}). \tag{13}$$

The MI and thus the CMI are 0 only if the subareas A and B do not exchange information and thus the species within them are not correlated. In the absence of intercorrelations, the CMI equals 0 (asynchronous regime), while for a positive CMI mutual dependence emerges, which corresponds to a synchronous regime.

In Fig. 7 the transition to synchronization is shown for two lattice sizes, $L = 512$ and 1024, using the SI and CMI. For sufficiently low probabilities, species mobility is insufficient to restrict the leading role of local reactions and thus the lattice is still poisoned. For slightly higher probabilities (e.g., $p_{ex} = 0.0003$) the lattice escapes poisoning states, however, distant areas remain asynchronous, resulting in very small positive values of the SI and CMI and thus very small correlations between them. Namely, a low rate of species mobility is inadequate to synchronize distant regions throughout the lattice. This is also depicted in Fig. 8, where the phase difference of two distant areas seems to follow a random walk for the same, small p_{ex}. Nevertheless, increasing p_{ex} further, e.g., to values of 0.0012 and 0.0014, correlations between distant areas also increase, which, however, may be lost after some time. This results in different dynamics of the phase difference, which now locks for long time intervals of almost-synchronous oscillations of species concentrations, but consecutively slips and locks in other intervals. These slips

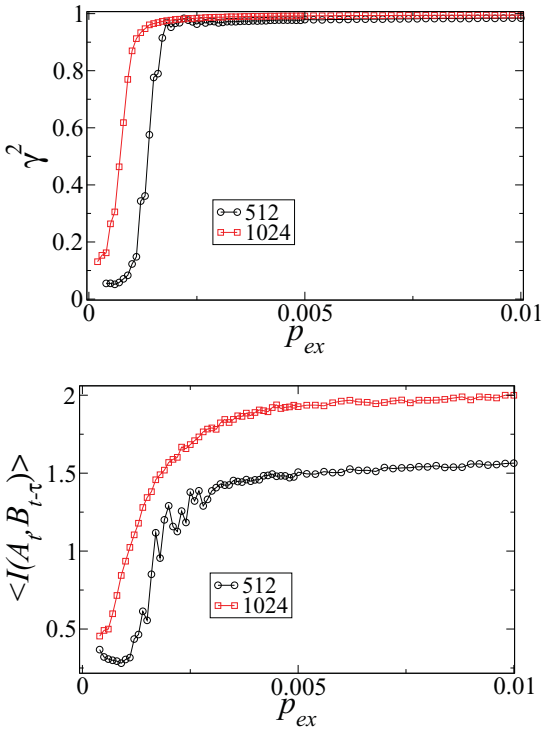

FIG. 7. (Color online) Transition to synchronization as represented by the SI and CMI with respect to the exchange probability p_{ex}. The exchange radius is $r_{ex} = 200$ sites and the remaining parameters are the same as in Fig. 5. Displayed points are the means over 10 different numerical experiments for the same initial configuration.

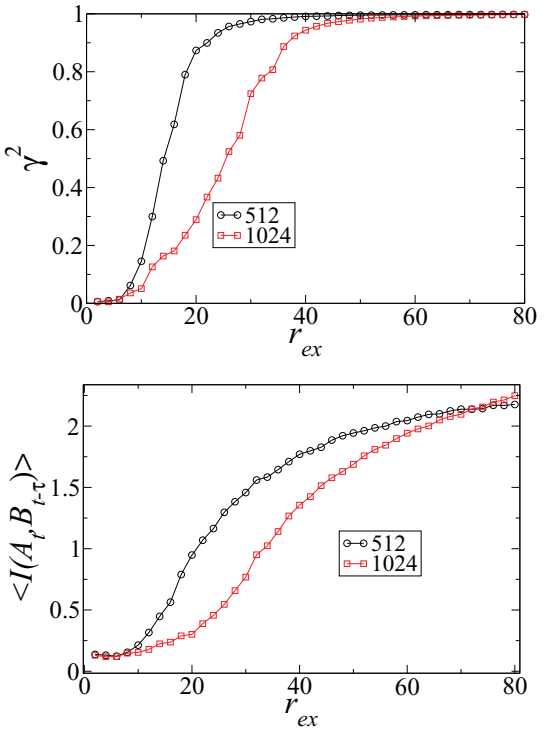

FIG. 9. (Color online) Transition to synchronization as represented by the SI and CMI with respect to the diffusion radius r_{ex}. The diffusion probability is $p_{ex} = 0.1$. The parameters k_i are the same as in Fig. 5. Displayed points are the means over 10 different numerical experiments for the same initial configuration.

appear rather often for lower values of p_{ex} and become rarer for higher p_{ex} values as shown in Fig. 8. Following this scenario, finally, the system is synchronized as shown in the same figure for $p_{ex} = 0.01$ and species oscillations coincide even in distant areas. The transition to synchronization, as shown in Fig. 7, is rather abrupt. Near the transition a typical intermittency crisis [17,32] is observed in the species oscillations appearing as rare phase slips.

A similar, but not the same, phase slip scenario is observed when the exchange radius increases for a constant probability p_{ex}. Figure 9 shows that for very small r_{ex} the species remain asynchronous even for large p_{ex}. Nevertheless, beyond a threshold of exchange probability, r_{ex} can drive the system to synchronization, which appears around $r_{ex} = 200$ as shown in Fig. 10. The latter results are presented here in order to supplement the whole picture of the dynamics where mobility plays a crucial role. Particularly, the exchange radius has been chosen as $r_{ex} = 200$ sites in all previous figures to ensure that the system can reach synchronization for p_{ex} values as small as 0.01.

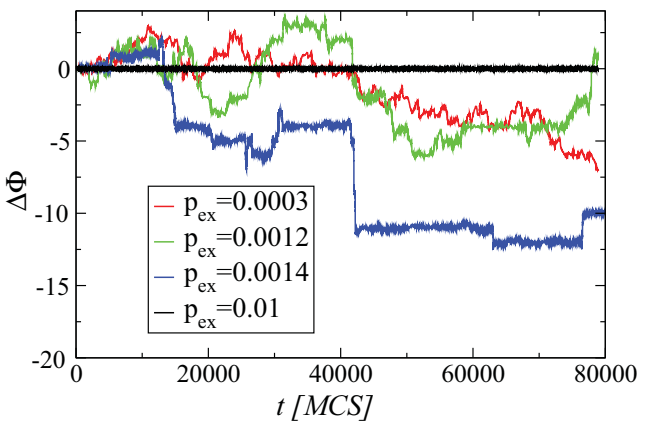

FIG. 8. (Color online) Phase difference dynamics shows a "phase slip" transition to synchronization. The corresponding probability p_{ex} is shown in the legend. The remaining parameters are the same as in Fig. 7.

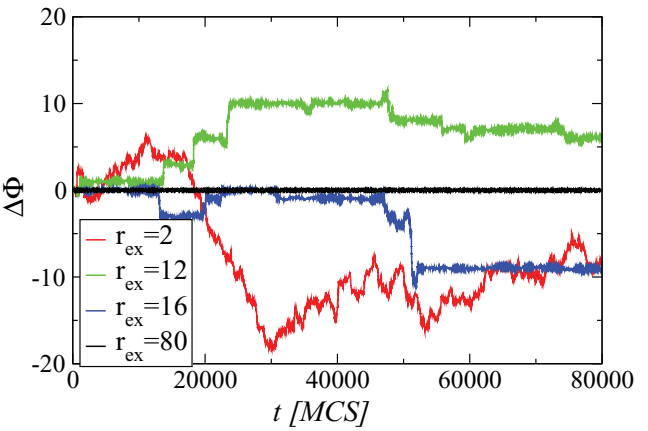

FIG. 10. (Color online) Phase difference dynamics. The corresponding exchange radius r_{ex} is shown in the legend. The remaining parameters are the same as in Fig. 9.

V. DISCUSSION

In this study a prototype ecosystem model and its route to synchronization are presented. This model consists of four species plus a fifth virtual species which corresponds to empty space in a cyclic domination. At the MF level, quasiperiodicity and chaos are the main dynamical aspects. Absorbing solutions which describe the survival of one species and the annihilation of the others are also observed in the MF. KMC simulations show that purely local reactions of immobile species drive the lattice to poisoning states. Both approaches converge only in the case where local rules are expanded to allow global reactions within the whole lattice. Namely, the "potential neighbors" are equiprobably chosen throughout the lattice instead of only the nearest sites, and then complete synchronization of all distant regions of the lattice is observed.

A different, gradually mixing mechanism that counterbalances the effects of local reactions is the long-distance exchange process. The probability of occurrence p_{ex} and the maximum range r_{ex} of this process change the mobility of species throughout the lattice. The system escapes poisoning states even for a weak mobility and is organized in a finite number of local oscillators, which in general are uncorrelated. Increasing species mobility results in better correlations between distant regions, and finally, synchronization arises. Near the transition to synchronization a typical intermittency crisis takes place, with the phase slips becoming more rare as the transition is approached. For the estimation of phase synchronization and interdependence, the SI and CMI, respectively, are used. Upon increasing the exchange probability, the SI increases abruptly (for small values of p_{ex}) and reaches unity, while the CMI also reaches a maximum, amplifying the scenario of phase synchronization. Finally, global and local oscillations coincide in phase and amplitude. A similar but less abrupt transition is observed as a function of r_{ex}, which also follows a phase slip scenario.

While our study has focused on the effects of long-distance exchange on the MF dynamics of the proposed chaotic model and its KMC square lattice implementation, future studies are needed to focus on species reactions taking place in complex and hierarchical networks, since the network architecture seems to play an important role in the stability of synchronous oscillations. The kinetic schemes which have been explored so far include conservative center-type, quasiperiodic, and chaotic dynamics. Other schemes which, at the MF level, present dissipative limit-cycle dynamics or weak chaos, appropriate for KMC simulations, need to be considered since the underlying MF dynamics seems also to play an equally important role in the development of synchronous, global oscillations.

ACKNOWLEDGMENTS

The authors thank E. Panagakou, L. Schimansky-Geier, and J. Kurths for fruitful discussions. N.K. acknowledges financial support through the National Center for Scientific Research "Demokritos."

[1] A. S. Pikovsky, M. G. Rosenblum, and J. Kurths, *Synchronization, A Universal Concept in Nonlinear Science* (Cambridge University Press, Cambridge, 2001).
[2] A. Arenas, A. Díaz-Guilera, J. Kurths, Y. Moreno, and C. Zhou, Phys. Rep. **469**, 93-153 (2008).
[3] B. Blasius, A. Huppert, and L. Stone, Nature **399**, 354 (1999).
[4] K. Wood, C. Van den Broeck, R. Kawai, and K. Lindenberg, Phys. Rev. E **75**, 041107 (2007).
[5] N. Kouvaris, F. Müller, and L. Schimansky-Geier, Phys. Rev. E **82**, 061124 (2010).
[6] M. Kuperman and G. Abramson, Phys. Rev. Lett. **86**, 2909 (2001).
[7] D. H. Zanette and M. Kuperman, Physica A **309**, 445 (2002).
[8] A. Efimov, A. V. Shabunin, and A. Provata, Phys. Rev. E **78**, 056201 (2008).
[9] J. S. Hansen, S. Toxvaerd, and E. Prstgaard, Physica D **177**, 31 (2003).
[10] Y. Kuramoto, *Chemical Oscillations, Waves and Turbulence* (Springer, Berlin, 1984).
[11] T. Vicsek, A. Czirok, E. Ben-Jacob, I. Cohen, and O. Shochet, Phys. Rev. Lett. **75**, 1226 (1995).
[12] E. M. Rauch and Y. Bar-Yam, Phys. Rev. E **73**, 020903(R) (2006).
[13] P. Romanczuk and U. Erdmann, Eur. Phys. J. Special Topics **187**, 127 (2010).
[14] M. Ballerini *et al.*, Proc. Natl. Acad. Sci. USA **105**, 1232 (2008).
[15] T. Reichenbach, M. Mobilia, and E. Frey, J. Theor. Biol. **254**, 368 (2008).
[16] N. Kouvaris and A. Provata, Eur. Phys. J. B **66**, 97 (2008).
[17] N. Kouvaris and A. Provata, Eur. Phys. J. B **70**, 535 (2009).
[18] E. Benincá *et al.*, Nature (London) **451**, 822 (2008).
[19] S. L. Pimm, *Food Webs* (Chapman and Hall, New York, 1982).
[20] J. D. Murray, *Mathematical Biology* (Springer, New York, 1993).
[21] G. Szabó, A. Szolnoki, and R. Izsák, J. Phys. A **37**, 2599 (2004).
[22] G. Szabó and G. Fáth, Phys. Rep. **446**, 97 (2007).
[23] T. Yanagita and A. S. Mikhailov, Phys. Rev. E **81** 056204 (2010).
[24] M. Paluš, Phys. Lett. A **235** 341 (1997).
[25] M. Paluš, V. Komárek, Z. Hrnčiř, and K. Štěrbová, Phys. Rev. E **63**, 046211 (2001).
[26] M. S. Baptista and J. Kurths, Phys. Rev. E **77**, 026205 (2008).
[27] N. Kouvaris, A. Provata, and D. Kugiumtzis, Phys. Lett. A **374**, 507 (2010).
[28] T. Pereia *et al.*, New J. Phys. **10**, (2008).
[29] F. M. Moukam Kakmeni and M. S. Baptista, Phys. Rev. AMANA–J. Phys.**70**, 1063 (2008).
[30] M. S. Baptista, S. P. Garcia, S. K. Dana, and J. Kurths, Eur. Phys. J. **165**, 119, 026205 (2008).
[31] D. Kugiumtzis, A. Papana, A. Tsimpiris, I. Vlachos, and P. G. Larsson, Lect. Notes Comput. Sci. **4345**, 298 (2006).
[32] A. Pikovsky, G. Osipov, M. Rosenblum, M. Zaks, and J. Kurths, Phys. Rev. Lett. **79**, 47 (1997).